Estimation of Harbor Responses due to Construction of a New Port in Ulsan Bay

Joong Woo LEE*· Hoon LEE**· Hak Sung LEE***· Min Su JEON****
*Division of Civil and Environmental System Engineering, Korea Maritime University, Busan 606-791, Korea
jwlee@mail.hhu.ac.kr
**Graduate School of Korea Maritime University, Busan 606-791, Korea
1vulcan98@hanmail.net
*** Ulsan Newport Container Terminal Corporation
y2kace2020@hanmail.net, Ulsan 680-160, Korea
****Undergraduate School of Korea Maritime University, Busan 606-791, Korea
minsuids@hotmail.com

Key Words: Coastal waters, Refraction and diffraction, Bottom friction, Breaking, Disaster prevention, Extended mild slope equation, Wave model, Energy redistribution,

ABSTRACT

Introduction of wave model, considered the effect of shoaling, refraction, diffraction, partial reflection, bottom friction, breaking at the coastal waters of complex bathymetry, is a very important factor for most coastal engineering design and disaster prevention problems. As waves move from deeper waters to shallow coastal waters, the fundamental wave parameters will change and the wave energy is redistributed along wave crests due to the depth variation, the presence of islands, coastal protection structures, irregularities of the enclosing shore boundaries, and other geological features. Moreover, waves undergo severe change inside the surf zone where wave breaking occurs and in the regions where reflected waves from coastline and structural boundaries interact with the incident waves. Therefore, the application of mild-slope equation model in this field would help for understanding of wave transformation mechanism where many other models could not deal with up to now. The purpose of this study is to form a extended mild-slope equation wave model and make comparison and analysis on variation of harbor responses in the vicinities of Ulsan Harbor and Ulsan New Port, etc. due to construction of New Port in Ulsan Bay. This type of trial might be a milestone for port development in macro scale, where the induced impact analysis in the existing port due to the development could be easily neglected.

1. INTRODUCTION

Wave field plays a very important role in all harbor and coastal projects. In most cases, however, a small amount of wave data from field observation are being used for engineering construction and planning. The reason for this is that field observation and physical modeling of waves are extremely difficult, costly, and time consuming. Since no wave gage installed at the site can anticipate future sea states, the desired sea-state information may be obtained and plans evaluated with reliable calibrated numerical models. Typically, the wave parameters are obtained from a wave transformation model that transfers the wave data collected at offshore deep water to the project site in the near shore. Until recently, the linear wave ray theory was used for wave transformation analysis by tracing rays from deep water to near shore. Because this theory assumes that wave energy propagates only along a ray, the effects on wave propagation of the wave height and direction along the wave crest are ignored. Therefore we can not apply this theory when wave ray crossings and caustics.

Starting in the early 1980's, coastal designers and researchers have recognized the importance of the combined effects of refraction and diffraction and begun to improve theories and associate them with numerical models. There are several wave theories available that could adequately describe the combined refraction and diffraction of waves from deep water to shallow water (Demirbilek and Webster, 1992). One of these is the mild-slope equation. Since the mild slope wave equation was initially solved by Berkhoff(1972) who used a finite element method, a more advanced form of the finite element method for water waves has been developed by Chen and Mei (1974). This is a depth-averaged, elliptic type partial differential equation which ignores locally emanated waves.

Numerous mild slope equation based numerical models have been developed for predicting the wave forces on offshore structures and studying wave fields along the coastline. A difficult problem in the prediction of waves near shore is to determine where approximately the wave breaking occurs when waves are inside the surf zone. In numerical models presently used, this location of breaking is not known a priori, and is usually selected with a criteria or a surf parameter based on the ratio of wave height to local water depth. Dissipation from the surrounding land boundaries and bottom friction may also be empirically incorporated into the extended mild slope equation models. A simplified version of the mild slope equation model is known as the parabolic

approximation model, which usually greatly reduces the excessive computational demands of mild slope equation model at the expense of further assumptions and simplifications which may render the numerical predictions inaccurate and inappropriate for many coastal and ocean engineering problems (Panchang et al., 1988). The parabolic approximation has been verified extensively by laboratory studies and field applications (Berkhoff et al. 1982), Liu and Tsay (1984), and Kirby and Dalrymple (1984). For details about parabolic approximation models, see Liu (1983), and Kirby and Dalrymple (1984).

Such models are hence applicable only to rectangular water domains for a very limited range of wave directions and frequencies. Most realistic coastal domains with arbitrary wave scattering cannot be modeled with these simplified models. While the extended mild slope equation model simulates the combined effects of wave refraction-diffraction, it also includes the effects of wave dissipation by friction, breaking, nonlinear amplitude dispersion, and harbor entrance losses.

2. BASIC THEORY

2.1 Basic Equations

In order to model surface gravity waves in coastal area, it is well accepted to use the two-dimensional elliptic mild-slope wave equation. The basic equation may be written as Equation (1):

$$\nabla\bullet(CC_g\nabla\eta)+\frac{C_g}{C}\sigma^2\hat{\eta}=0 \tag{1}$$

where $\hat{\eta}(x,y)$ =complex surface elevation function, from which the wave height can be estimated, σ =wave frequency under consideration (in radians/second), C(x,y) = phase velocity = σ/k, Cg(x,y) = group velocity = $\frac{\partial\sigma}{\partial k}=nC$ with $n=\frac{1}{2}\left(1+\frac{2kd}{\sinh 2kd}\right)$, k(x,y) = wave number (= 2π/L), related to the local depth d(x,y) through the linear dispersion relation: $\sigma^2 = gk\tanh(kd)$. Equation (1) simulates wave refraction, diffraction, and reflection in coastal domains of arbitrary shape. However, various other mechanisms also influence the behavior of waves in a coastal area. The mild-slope equation can be extended as follows to include the effects of bottom friction and dissipation due to wave breaking.

$$\nabla\bullet\left(CC_g\nabla\hat{\eta}\right)+\left(\frac{C_g}{C}\sigma^2+i\sigma w+iC_g\sigma\gamma\right)\hat{\eta}=0 \tag{2}$$

where w is a friction factor and γ is a wave breaking parameter. We have used the following form of the damping factor, following Dalrymple et al. (1984).

$$w=\left(\frac{2n\sigma}{k}\right)\left[\frac{2f_r}{3\pi}\frac{ak^2}{(2kd+\sinh 2kd)\sinh kd}\right] \tag{3}$$

where $a(=H/2)$ is the wave amplitude and f_r is a friction coefficient. The friction coefficient depends on the Reynolds number and the bottom roughness. We referred Madsen (1976) and Dalrymple et al. (1984). Typically, values for f_r are in the same range as for Manning's dissipation coefficient 'n', specified as a function of (x,y) assigning larger values for elements near harbor entrances to consider entrance loss. For the wave breaking parameter γ, we use the following formulation (Dally et al., 1985; Demirbilek, 1994).

$$\gamma=\frac{0.15}{d}\left(1-\frac{0.16d^2}{4a^2}\right) \tag{4}$$

In addition to the above relationships, simulation of nonlinear waves may be conducted by using the mild slope equation. This is accomplished by incorporating amplitude-dependent wave dispersion, which has been shown to be important in certain situations. Equaion (5) is rearranged to include the nonlinear dispersion relation used in place of Equation (1) through (3).

$$\sigma^2=gk\left[1+(ka)^2F_1\tanh^5 kd\right]\tanh\left\{kd+kaF_2\right\} \tag{5}$$

where $F_1 = \dfrac{\cosh(4kd) - 2\tanh^2(kd)}{8\sinh^4(kd)}$

$F_2 = \left(\dfrac{kd}{\sinh(kd)}\right)^4$ (6)

2.2 Boundary Conditions

No flow normal to the surface of rigid, impermeable vertical walls gives $\partial\eta/\partial n = 0$. However, for coastlines or permeable structures, the following partial reflection boundary condition applies along

$$\frac{\partial \eta}{\partial n} = \alpha\hat{\eta} \tag{7}$$

where α is a complex coefficient, which is generally represented as Equation (8).

$$\alpha = ik\frac{1-K_r}{1+K_r} \tag{8}$$

where K_r is the reflection coefficient. Along the open boundary where outgoing waves must propagate to infinity, the Sommerfeld radiation condition applies

$$\lim_{kr\to\infty}\sqrt{kr}\left(\frac{\partial}{\partial r} - ir\right)\hat{\eta}_s \to 0 \tag{9}$$

where $\hat{\eta}_s$ is the scattering wave potential. It is shown in Mei (1983) that the desired scattered wave potential $\hat{\eta}_s$, which is a solution of the mild-slope equation and satisfies the radiation condition Equation (9), can be written as Equation (10).

$$\hat{\eta}_s = \sum_{n=0}^{\infty} H_n(kr)(\alpha_n \cos n\theta + \beta_n \sin n\theta) \tag{10}$$

where $H_n(kr)$ are the Hankel functions of the first kind. The Hankel functions of the second kind do not satisfy the Sommerfeld radiation condition at infinity and are hence excluded from (10). However, the $\hat{\eta}_s$ given in Equation (10) requires that the exterior domain related to coastline A1 and A2 in Fig. 1 be of constant depth. Also for harbor problems, the scattered wave potential as described by (10) demands straight, collinear and fully reflective coastlines in the exterior region. To overcome these problems, Xu et al. (1996) have developed a parabolic approximation in dealing with the open boundary as follows.

$$\frac{\partial \eta_s}{\partial r} + p\hat{\eta}_s + q\frac{\partial \hat{\eta}_s}{\partial \theta^2} = 0 \tag{11}$$

where $p = (k^2r^2 + k_0^2r^2 + ik_0r + 1/4)/(2ik_0r^2)$, $q = 1/(2ik_0r^2)$. k_0 can be taken as the wave number corresponding to the averaged water depth along the open boundary Γ. Within the model domain Ω, the extended mild slope equation applies. The parabolic approximation (11) will be used only along the semi-circular arc Γ as the open boundary condition.

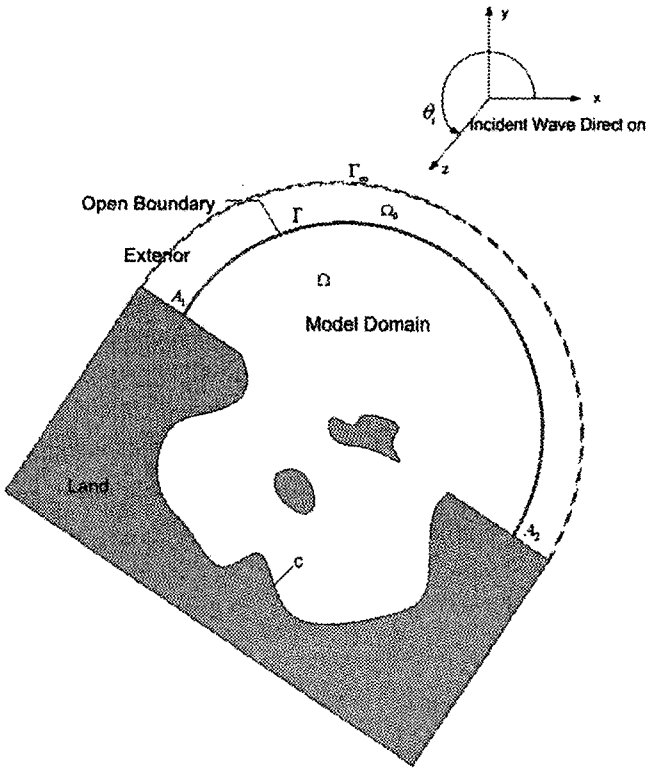

Fig. 1 Definition sketch of model domain and boundary

3. NUMERICAL MODEL FORMULATION

The extended mild slope equation such as Equation (2) is an integrated wave transformation equation which considers the effect of shoaling, refraction, diffraction, partial reflection, bottom friction, breaking at the coastal waters of complex bathymetry. In this study, we use the hybrid element method, which is a powerful approach for modeling coastal responses in regions of complex shaped harbor as in Fig. 1. In the case of a group of coastal boundaries surrounded by an open sea of constant depth, the incident wave may be written as (Demirbilek and Gaston, 1985).

$$\hat{\eta}_I = Ae^{ikr\cos(\theta-\theta_I)} = A\sum \varepsilon_n i^n J_n(kr)\cos n(\theta-\theta_I) \tag{12}$$

where A is the amplitude of the incident wave, θ_I is the incident wave angle with respect to the x-axis, J_n is the n-th order Bessel functions of the first kind. When n=0, ε_n=1, and when n$\neq$ 0, ε_n=2.

As shown in Fig. 1, the entire domain is divided into two sub-domains, a finite inner domain Ω and an infinite outer domain Ω_0. Domain Ω is the numerical model domain. Domain Ω_0 is the exterior domain extending to infinity. We assume that complicated topography, structures, and islands, are located inside the circular boundary Γ in domain Ω. The total wave potential in Ω_0 can be written as the sum of incident wave potential and the scattered wave potential as shown in Equation (13).

$$\hat{\eta}_{ext} = \hat{\eta}_I + \hat{\eta}_S \tag{13}$$

We can write the governing Equation (2) in the general form of Equation (14) for abbreviation.

$$\nabla\cdot(\tilde{\alpha}\nabla\hat{\eta}) + \tilde{b}\hat{\eta} = 0 \tag{14}$$

where $\tilde{a} \equiv CC_g$ and $\tilde{b} \equiv n\sigma^2 + i\sigma\omega + iC_g\sigma\gamma$. The exterior wave field is written as $\hat{\eta}_{ext} = \hat{\eta}_I + \hat{\eta}_R + \hat{\eta}_S$, where $\hat{\eta}_I$, $\hat{\eta}_R$, and $\hat{\eta}_S$ represent the incident, the reflected, and the scattered wave fields, respectively. Based on the assumptions, we can rearrange such as in Equation (15).

$$\hat{\eta}_{ext} = 2A\sum_{n=0}^{\infty} \varepsilon_n i^n J_n(kr)\cos\theta_I \cos n\theta + \sum_{n=0}^{\infty} H_n(kr)\alpha_n \cos n\theta \tag{15}$$

Applying above equation to the governing equation and after proper assembling through Galerkin finite element formulation with boundary conditions, finally we come to the general form of algebraic equation as Equation (16).

$$[A]\{\hat{\eta}\} = \{f\} \tag{16}$$

Equation (16) is the desired linear system of equations, which is the hybrid element representation of the extended mild slope equation for open sea problems. Notice that the boundary conditions, including coastline boundaries and the semi-circular open boundary, are all assembled in Equation (16). In order to solve the elliptic mild slope equation, the problem has to be solved simultaneously over the entire domain. This leads to a very large linear system of equations. Direct methods are inapplicable due to extremely large storage requirement of the matrix [A]. Iterative methods, on the other hand, require memory for only the non-zero elements in [A] and found to be far more efficient. Therefore, we used iterative methods from studies of Panchang et al. (1991) and Li (1994) for the present study.

4. NUMERICAL SIMULATION AND ANALYSIS

Ulsan harbor is one of the biggest industrial harbor in Korea and naturally superior harbor located at southeastern edge of the Korean Peninsula. And it's 58Km in total length of coastline, 83㎢ in water dimension within the harbor, (-)4 ~ (-)27m in the depth of water. Ulsan harbor is strategically important harbor for domestic base industries. There is Taehwa River across Ulsan metropolitan city and Origin Ulsan harbor, Onsan harbor, and Mipo harbor consist of the current Ulsan harbor. Now it's domestic base harbor processing 15.8% of logistics, 36.95% of oil, and 61% of trading volume with North Korea as well as the biggest harbor supporting energy supply in Korea. The capability to come alongside quay simultaneously is 91ships and 3,154,000 DWT(quay wall extension is 15,281m). Ulsan harbor is expected to support domestic base industries as the biggest industrial harbor in Korea by developing 32 units additionally till year 2011. Moreover, 24 units are expected to be developed additionally till year 2020 after year 2011. The location and water depth of Ulsan Bay and harbor

facilities are shown in Fig. 2 and Fig. 3. The present study includes the extension of breakwaters and land reclamations at Onsan harbor and at the entrance of the Original Ulsan harbor. Additional gaps were included midway along the length of both north and south sides of the new breakwater to improve water circulation and navigation. Because of its orientation, storm waves may cause substantial damage or hazard. From this viewpoint, we tried to analyze and predict wave heights and directions in- and out-side the harbor to determine if there are any significant differences between the two configurations.

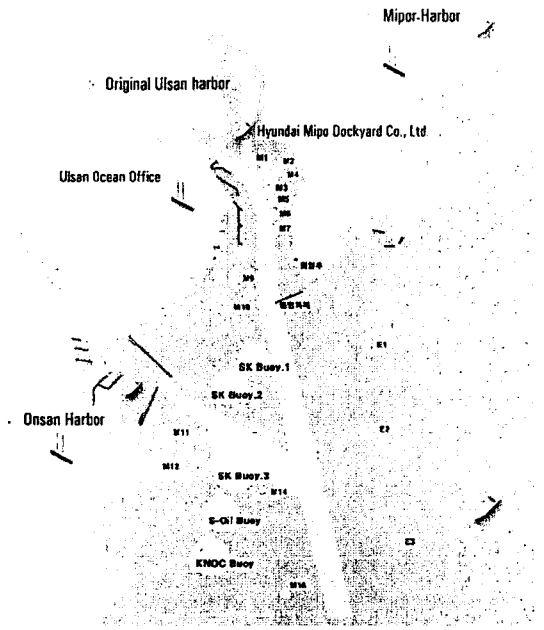

Fig. 2 Location map and limit of Ulsan harbor

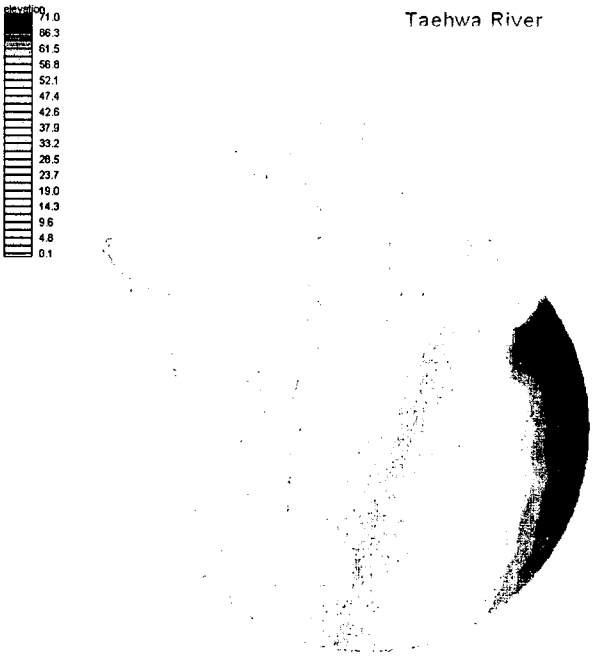

Fig. 3 Water depth at the model site

4.1 Input Condition

Fig. 3 also shows the orientation of the model domain relative to Original Ulsan harbor and Onsan harbor. Since the harbor area is large and wave periods as small as 8 and 10 secs are prevalent as shown in Table 1, we came to Table 2 to meet the required grid size (model requires a minimum 6 to 10 elements per wavelength. The mesh for present harbor contains a total of 143,441 elements and 73,588 nodes, whereas a total of 140,377 elements and 72,143 nodes for the New port project. Fig. 4 and Fig. 5 show the mesh details in vicinity of breakwaters and public piers. Bathymetric data were collected from engineering Co., Ltd. and the numerical chart. Eight different cases, composed of two wave periods and two wave directions, were selected for study based on harbor orientation (see Table 3). In this table, we define linear and non-linear terms for dispersion relationship and break term for wave breaking formulation. Waves traveling to the west and the north harbor are most likely to affect Onsan harbor and Original Ulsan harbor, respectively, since they have a clear path through the breakwater gap. Because the local interest was in the areas of Onsan harbor and Original Ulsan harbor, two transects (0 and 1) were selected.

Table 1 Incident wave condition for design wave

Wave				
Direction	Height	Period	Return Period	Remark
S	6.4m	10 sec	50 year	MOMAF, Typhoon VERA(1986)
E	4.8m	8 sec	50 year	MOMAF, REPORT

Table 2 Numerical model characteristics

Case	Number of Elements	Number of Nodes	Calculation Times (P4 2.6GHz, 512Mb)
Present	143,441	73,588	114 min.
After New port Project	140,377	72,143	100 min.

Table 3 Simulation conditions

Port Project	Case	Wave Condition
Before the New port project	Case 1	linear
	Case 2	linear-break
	Case 3	nonlinear
	Case 4	nonlinear-break
After the New port project	Case 5	linear
	Case 6	linear-break
	Case 7	nonlinear
	Case 8	nonlinear-break

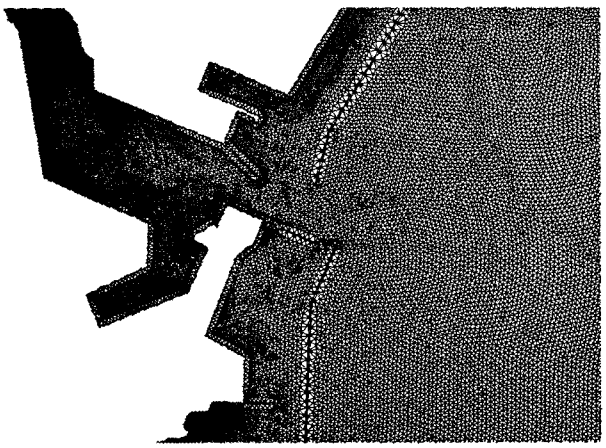

Fig. 4 Details of finite element mesh for Onsan harbor

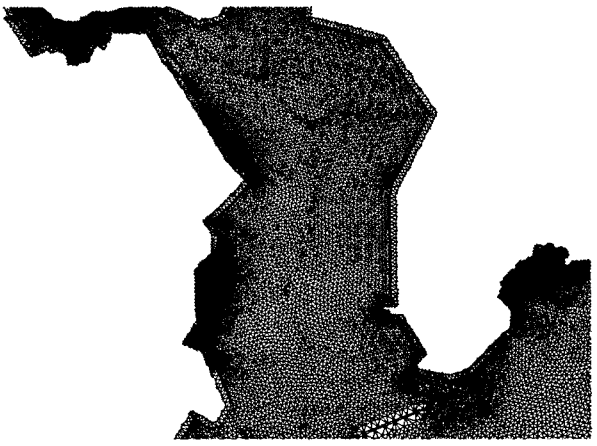

Fig. 5 Details of finite element mesh for Original Ulsan harbor

Transect 0 goes to Onsan harbor and transect 1 goes to Original Ulsan harbor. Fig. 6 show the orientation of these two transects for the present and the New port project at Onsan harbor, respectively. The two transects provide a general overview of wave height inside and outside of harbors, Original Ulsan harbor and Onsan harbor. However, because of the significant variability in wave height along each one as a function of position and water depth, it is difficult to compare wave energy between the two configurations based on the responses along these transects.

4.2 Results and Analyses

Fig. 7 and Fig. 8 are contour plots of the wave height for 10 seconds of wave period and traveling to the north direction for the present harbor and the Onsan harbor project, respectively. The contours illustrate the same wave heights within the domain. The incident wave height is 6.4 m on the offshore boundary and decreases as waves propagate into the harbor. Larger wave heights occur to Original Ulsan harbor. However, the narrow gap after Onsan outer breakwaters construction significantly reduces wave energy inside the Original Ulsan harbor. Fig. 9 and Fig. 10 are contour plots of the wave height for 8 seconds of wave period and traveling to the west direction for the present harbor and the Onsan harbor project, respectively. The incident wave height is 4.8 m on the offshore boundary and decreases as waves propagate into the harbor. Larger wave heights for this case occur to Onsan harbor. The wave patterns are similar for the longer wave periods, and display slightly different penetration patterns of wave energy.

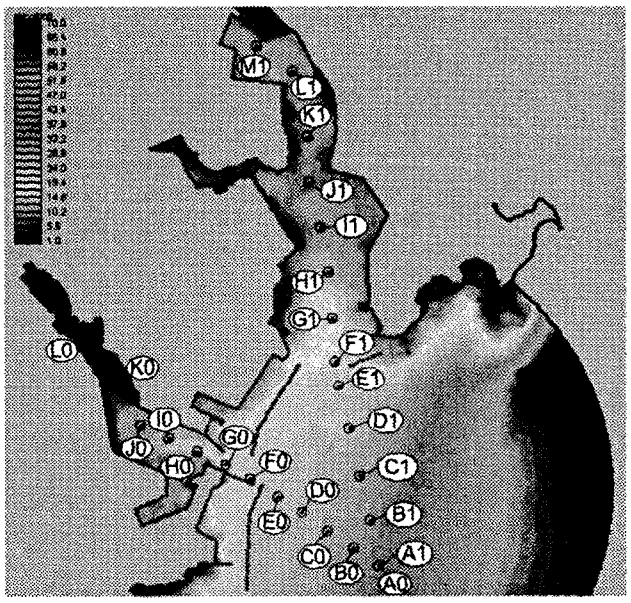

Fig. 6 Orientation of transect lines (0, 1) for Ulsan harbor

Because the gap of breakwaters of Onsan harbor is not changed after outer breakwaters(about 400 m gap), there is no significant wave energy variation inside the harbor. As a base case, we ran a "no-breakwater" case of Onsan harbor before the breakwater was constructed. We found that the existing north breakwater of Onsan harbor reduce the incoming wave heights by as much as 75% percent versus a 250m cut off breakwater condition. All figures are resulted from the nonlinear dispersion and breaking condition simulation.

Fig. 11 through Fig. 18 show the predicted wave heights along each transect for different model simulation cases. Linear dispersion condition shows the highest responses along the whole transect. The responses before the New port project show rapid reduction of amplification factors at station G. On the other hand, the rapid reduction responses after the New port project show at station F. That's because of the construction of outer breakwaters at the entrance of Onsan harbor. Wave breaking mechanism contributes significantly to the harbor responses. As per model experiment with an elliptic shoal, nonlinear dispersion reduces the peaks but raises the trough of response. For linear dispersion, breaking reduces the response by half but for nonlinear dispersion, this trend is changed a little bit. The results from nonlinear dispersion and breaking wave condition fit well with the one from the steady

state spectral wave (STWAVE) model with wind effect considered. However, the STWAVE model is appropriate for open coast and deepwater applications, and may not be suitable for shallow depths where diffractions, reflection, and nonlinear dispersion could be important.

Fig. 7 Wave height predictions for the present configuration with wave conditions of 6.4 m and 10 sec, and wave direction of S (Nonlinear dispersion and wave breaking condition)

Fig. 8 Wave height predictions for the New port project with wave conditions of 6.4 m and 10 sec, and wave direction of S (Nonlinear dispersion and wave breaking condition)

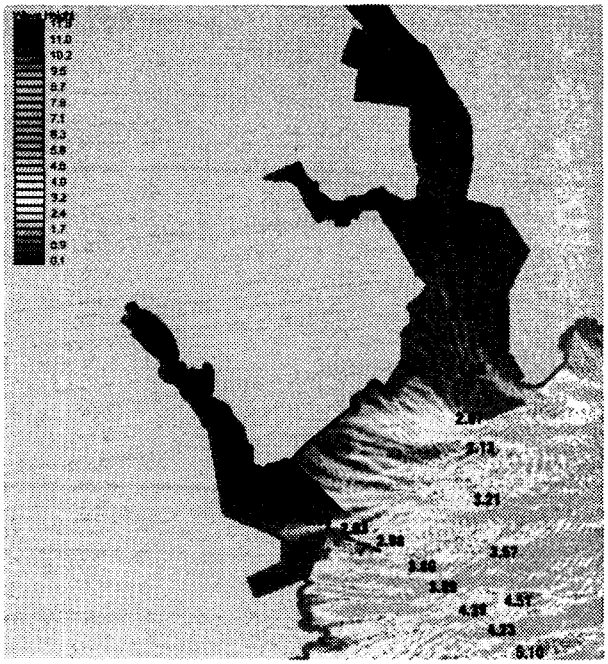

Fig. 9 Wave height predictions for the present configuration with wave conditions of 4.8 m and 8 sec, and wave direction of E (Nonlinear dispersion and wave breaking condition)

Fig. 10 Wave height predictions for the New port project with wave conditions of 4.8 m and 8 sec, and wave direction of E (Nonlinear dispersion and wave breaking condition)

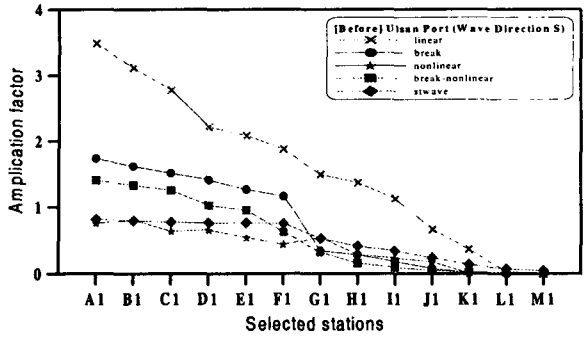

Fig. 11 Amplification factors of Original Ulsan harbor before construction of New port in Ulsan Bay (Wave direction : S)

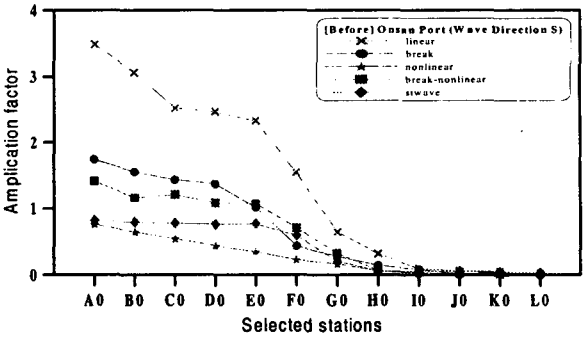

Fig. 12 Amplification factors of Onsan harbor before construction of New port in Ulsan Bay (Wave direction : S)

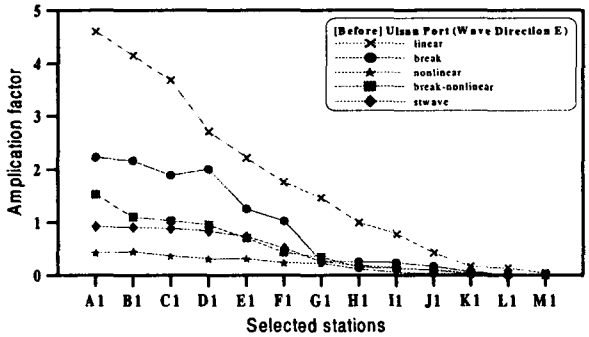

Fig. 13 Amplification factors of Original Ulsan harbor before construction of New port in Ulsan Bay (Wave direction : E)

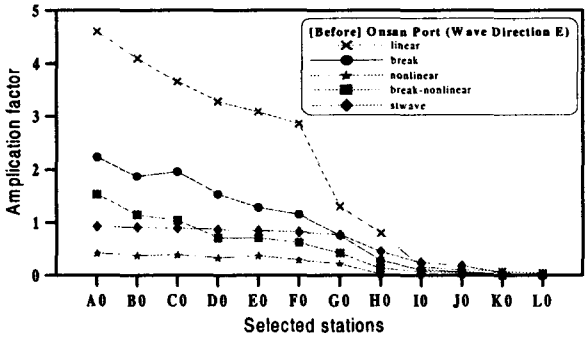

Fig. 14 Amplification factors of Onsan harbor before construction of New port in Ulsan Bay (Wave direction : E)

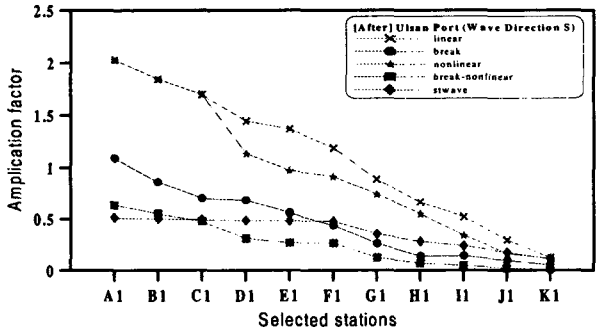

Fig. 15 Amplification factors of Original Ulsan harbor after construction of New port in Ulsan Bay (Wave direction : S)

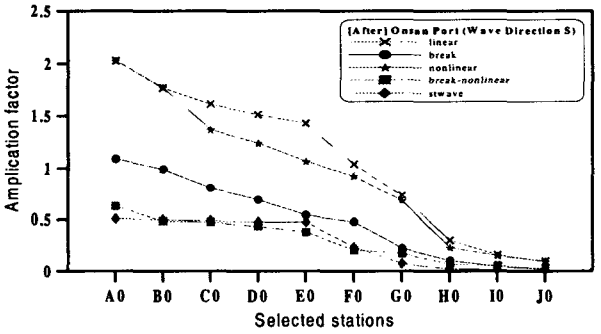

Fig. 16 Amplification factors of Onsan harbor after construction of New port in Ulsan Bay (Wave direction : S)

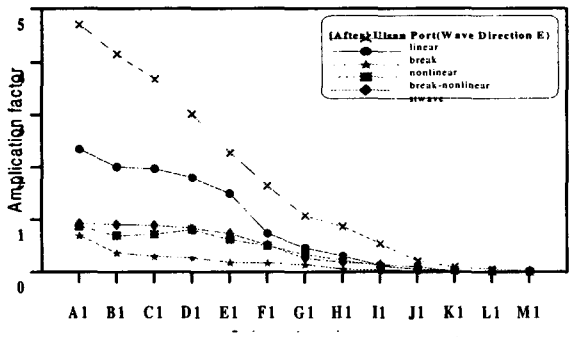

Fig. 17 Amplification factors of Original Ulsan harbor after construction of New port in Ulsan Bay (Wave direction : E)

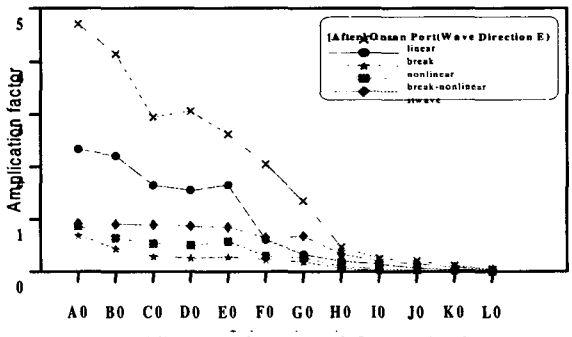

Fig. 18 Amplification factors of Onsan harbor after construction of New port in Ulsan Bay (Wave direction : E)

5. SUMMARY AND CONCLUSIONS

This study has described results from the extended mild-slope equation model simulation for predicting wave heights in Ulsan Bay, Korea. New outer breakwaters at Onsan harbor were constructed with an existing as-built gap of 400m between the breakwater sections on either side of the entrance, comparing with the original gap of 25m. Furthermore, the gap of the entrance for Original Ulsan harbor was reduced to 600m due to construction of the north outer breakwater at Onsan harbor. Wave height predictions from the numerical model were compared between the two configurations. A series of 16 wave conditions as shown in Table 1 and Table 3 were selected as representative wave conditions in Ulsan Bay. Predicted wave heights were compared along two transects (0, 1) from offshore to the innermost basins.

For the existing configuration, larger wave heights occur to the north end channel of Original Ulsan harbor for south waves, to the west end and northwest channel of Onsan harbor for east waves. For construction configuration, the narrower gap reduces waves traveling to the north more than to the west along both transects. Due to construction of new port at Onsan harbor side, the variation of harbor responses in the Original Ulsan harbor shows up to a noticeable level. In this case the variation occurred in a way of wave height reduction to the harbor basin but induces difficulties to the ship passage at or outside the entrance. Among several model analyses, the nonlinear and breaking wave conditions are showed the most applicable results.

Comparisons with the extended mild-slope equation model study are in general agreement with the wave heights and directions predicted by STWAVE model.

REFERENCES

Berkhoff, J. C. W. (1972). Computation of Combined Refraction – Diffraction, Proc. 13th International Coastal Engineering Conference, 741-790.

Chen, H. S. and Mei, C. C. (1974). Oscillation and Wave Forces in a Man-made Harbor in the Open Sea, Proc. 10th Naval Hydrodynamics Symposium, 573-596.

Dally, W. R., Dean, R. G., and R. A. Dalrymple, R. A. (1985). Wave Height Variation across Beaches of Arbitrary Profile, J. Geophys. Research, **90**, 1917-11927.

Dalrymple, R. A., Kirby, J. T., and Hwang, P. A. (1984). Wave Diffraction due to areas of high energy dissipation, J. Waterway, Port, Coastal and Ocean Eng., **110**, 67-79.

Demirbilek, Z. (1994). Comparison Between REFDIFS and CERC Shoal Laboratory Study, Unpublished Report, Waterways Exp. Station, Vicksburg, MS, p 53.

Demirbilek, Z. and Gaston, J. D. (1985). Nonlinear Wave Loads on a Vertical Cylinder, Ocean Eng., **12**, 375-385.

Demirbilek, Z. and Webster, W. C. (1992). Application of the Green-Naghdi Theory of Fluid Sheets to Shallow-water Wave Problems, Report 1: Model Development, Report 2: User's Manual and Examples for GNWAVE, U.S. Army Waterways Exp. Station, Tech. Reports CERC-92-1 and CERC-92-13, Vicksburg, MS.

Kirby, J. T. and Dalrymple, R. A. (1984). Verification of a Parabolic Equation for Propagation of Weakly-Nonlinear Waves, Coastal Engineering, **8**, 219-232.

Li, B. (1994). A Generalized Conjugate Gradient Model for the Mild Slope Equation, Coastal Engineering, **23**, 215-225.

Liu, P.L.-F. (1983). Wave-Current Interactions on a Slowly Varying Topography, J. Geophys. Research, **88**, 4421-4426.

Liu, P. L.-F. and Tsay, T. K. (1984). Refraction-Diffraction Model for Weakly Nonlinear Water Waves, J. Fluid Mech., **141**, 265-274.

Madsen, O.S. (1976). Wave Climate of the Continental Margin: Elements of its Mathematical Description, Marine Sediment Transport and Environmental Management (eds. D. Stanley and D.J.P. Swift), John Wiley, New York, 65-87.

Mei, C. C. (1983). The Applied Dynamics of Ocean Surface Waves, John Wiley, New York.

Panchang, V. G., Cushman-Roisin, B., and Pearce, B. R. (1988). Combined Refraction-Diffraction of Short Waves for Large Coastal Regions, Coastal Engineering, **12**, 133-156.

Panchang, V. G., Ge, G., Cushman-Roisin, B., and Pearce, B. R. (1991). Solution to the Mild-Slope Wave Problem by Iteration, Applied Ocean Research, **13**, 187-199.

Xu, B., Panchang, V. G., and Demirbilek, Z. (1996). Exterior Reflections in Elliptic Harbor Wave Models, J. Waterway, Port, Coastal, and Ocean Engr., **122**, 118-126.